

# Low Wall Shear Stress Is Associated with Local Aneurysm Wall Enhancement on High-Resolution MR Vessel Wall Imaging

W. Xiao, T. Qi, S. He, Z. Li, S. Ou, G. Zhang, X. Liu, Z. Huang, and F. Liang



## ABSTRACT

**BACKGROUND AND PURPOSE:** Some retrospective studies have found that the aneurysm wall enhancement on high-resolution MR vessel wall postgadolinium T1WI has the potential to distinguish unstable aneurysms. This study aimed to identify hemodynamic characteristics that differ between the enhanced and nonenhanced areas of the aneurysm wall on high-resolution MR vessel wall postgadolinium T1WI.

**MATERIALS AND METHODS:** TOF-MRA and high-resolution MR vessel wall T1WI of 25 patients were fused to localize the enhanced area of the aneurysm wall. Using computational fluid dynamics, we studied the aneurysm models. Mean static pressure, mean wall shear stress, and oscillatory shear index were compared between the enhanced and nonenhanced areas.

**RESULTS:** The aneurysmal enhanced area had lower wall shear stress ( $P < .05$ ) and a lower oscillatory shear index ( $P = .021$ ) than the nonenhanced area. In addition, the whole aneurysm had lower wall shear stress ( $P < .05$ ) and a higher oscillatory shear index ( $P = .007$ ) than the parent artery.

**CONCLUSIONS:** This study suggests that there are hemodynamic differences between the enhanced and nonenhanced areas of the aneurysm wall on high-resolution MR vessel wall postgadolinium T1WI.

**ABBREVIATIONS:** HR-VWI = high-resolution MR vessel wall imaging; OSI = oscillatory shear index; P = mean static pressure; WSS = wall shear stress

An intracranial aneurysm is regarded as the most common culprit for nontraumatic subarachnoid hemorrhage, a devastating clinical situation that is usually followed by the risks of aneurysm rebleeding, cerebral vascular spasm, and hydrocephalus. Imaging examinations, one of which is high-resolution MRI, have been used to discover, diagnose, estimate, and evaluate aneurysms. For instance, as a noninvasive examination, high-resolution MRI can be used as a screening method and a tool for follow-up visits, and it can help visualize dissecting aneurysms.<sup>1</sup> Moreover, it can be used to evaluate the depth of aneurysm location before open surgery such as the clipping of middle cerebral bifurcation aneurysms. In patients with subarachnoid hemor-

rhage and multiple aneurysms, MR imaging can help discriminate the responsible aneurysm. Fu et al<sup>2</sup> proposed that circumferential aneurysmal wall enhancement on high-resolution MR vessel wall imaging (HR-VWI) is correlated with headaches and third nerve palsy caused by unruptured aneurysms. Two previous studies indicated that as an indicator of inflammation, the aneurysm wall enhancement on HR-VWI postgadolinium T1WI has the potential for discriminating unstable aneurysms from stable ones.<sup>3,4</sup> Wang et al<sup>5</sup> found that all partial wall enhancement of 16 aneurysms was in the irregularly shaped portions or daughter sacs in their study.

Computational fluid dynamics has been used to investigate hemodynamic parameters that are linked with cerebral aneurysm formation, progression, and rupture, one of which is wall shear stress (WSS), the most highlighted but controversial parameter.<sup>6-8</sup> However, to our knowledge, no published investigations have revealed the association between hemodynamic characteristics and aneurysm wall enhancement on HR-VWI postgadolinium T1WI.

Therefore, we designed a retrospective study into hemodynamic parameters on aneurysm models with local wall enhancement on HR-VWI postgadolinium T1WI, to provide a new idea for the future investigation into wall enhancement.

Received May 3, 2018; accepted after revision July 30.

From the Departments of Neurosurgery (W.X., T.Q., S.O., G.Z., X.L., Z.H., F.L.) and Radiology (S.H., Z.L.), The First Affiliated Hospital, Sun Yat-sen University, Guangzhou, China.

Weiping Xiao and Tiewei Qi contributed equally to this work.

Please address correspondence to Feng Liang, MD, First Affiliated Hospital of Sun Yat-sen University, Department of Neurosurgery, 58 Zhongshan Er Rd, Guangzhou, Guangdong, 510080, China; e-mail: liangf6@mail.sysu.edu.cn



Indicates article with supplemental on-line appendix and table.



Indicates article with supplemental on-line photos.

<http://dx.doi.org/10.3174/ajnr.A5806>

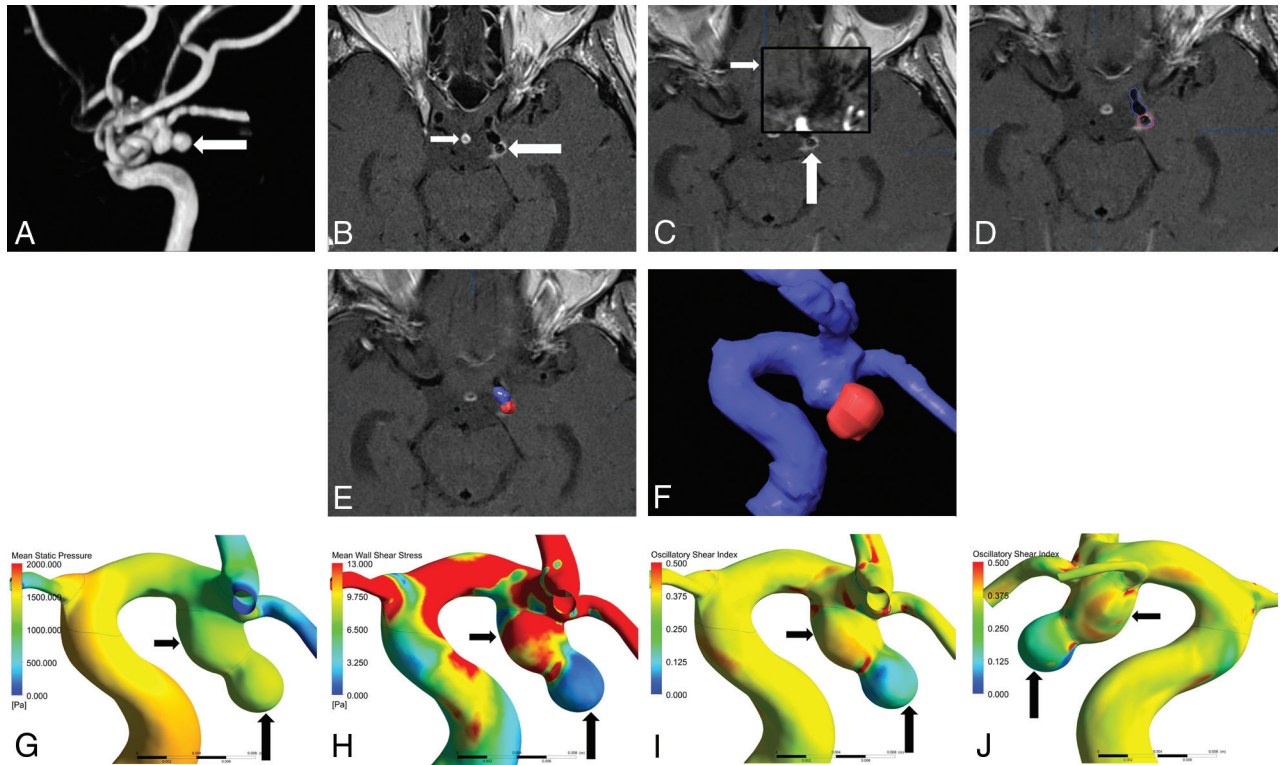


**FIG 1.** A, MRA shows a posterior communicating artery aneurysm (*white arrow*). B, Local enhancement on the aneurysmal wall on HR-VWI postgadolinium T1WI (*large white arrow*) compared with that of the pituitary infundibulum (*small white arrow*). C, Auto Fusion of HR-VWI T1WI (*large white arrow*) and TOF-MRA (*small white arrow*) images. D–F, Location of the enhanced area (highlighted in red) on the aneurysm (displayed in blue). G, Mean static pressure distribution. H, WSS distribution. The enhanced area has lower mean WSS (*large black arrow*) than the nonenhanced area (*small black arrow*). I and J, OSI distribution. The enhanced area has lower OSI (*large black arrow*) than the nonenhanced area (*small black arrow*).

## MATERIALS AND METHODS

### Patient Selection

This retrospective study protocol was approved by the ethics committees of the First Affiliated Hospital, Sun Yat-sen University, and informed consent was exempted. Patients with aneurysms who underwent an HR-VWI examination before an operation or conservative treatment from January 2015 to March 2016 were reviewed. The inclusion criteria were as follows: 1) intracranial aneurysms diagnosed by CTA, MRA, or DSA; 2) anterior circulation aneurysms; 3) HR-VWI postgadolinium T1WI revealing wall enhancement; and 4) available HR-VWI and DSA 3D rotational angiography data. The exclusion criteria were the following: 1) fusiform, dissecting aneurysms or pseudoaneurysms; 2) anterior communicating artery aneurysms or posterior circulation artery aneurysms; and 3) HR-VWI and 3D rotational angiography data unavailable.

### Imaging Analysis

Two experienced neurovascular radiologists (with >5 years' experience in neurovascular imaging) analyzed pre- and postcontrast T1-weighted images, retrospectively and respectively, to determine whether there was local enhancement. They were blinded to the patients' clinical data and other sequences except for 3D-TOF imaging before the analysis. Discordance between 2 readers was resolved by consensus. One of the readers performed a second analysis after 3 weeks. By comparing pre- and postcontrast T1WI, we defined the wall enhancement as circumferential when the whole aneurysm wall was enhanced after contrast agent infusion;

otherwise, it was defined as partial when only part of the aneurysm wall was enhanced. Only aneurysms with local enhancement were enrolled into this study. Protocols of HR-VWI and 3D rotational angiography are provided in the On-line Appendix.

### Location of Aneurysm Wall Enhanced Area

DICOM files of HR-VWI were imported into iPlan cranial 3.0 (BrainLab, Munich, Germany). Then, in the projection of Image Fusion, the HR-VWI T1WI and TOF-MRA images were chosen and paired (Fig 1C and Fig 2C). They were then merged using the function of Auto Fusion. After Auto Fusion, merged images were checked on the axial view and fine manual fusion was performed for tiny adjustments, which ensured the precision of Image Fusion. Aneurysm models were reconstructed with TOF-MRA using Auto Segmentation. Irrelevant arteries were cut off manually, with aneurysms, parent arteries, and the important branches preserved. Aneurysm wall enhanced areas were also reconstructed using manual segmentation with T1WI (Fig 1D and Fig 2D). The aneurysm models and aneurysm wall enhanced area were displayed simultaneously to locate the enhanced area (Fig 1E, -F and Fig 2E, -F).

### Aneurysm Modeling

The patients' 3D rotational angiography DICOM files were imported into Mimics 17.0 (Materialise, Leuven, Belgium) for a rough model reconstruction by threshold segmentation. Then the unconnected regions were manually removed with the region-

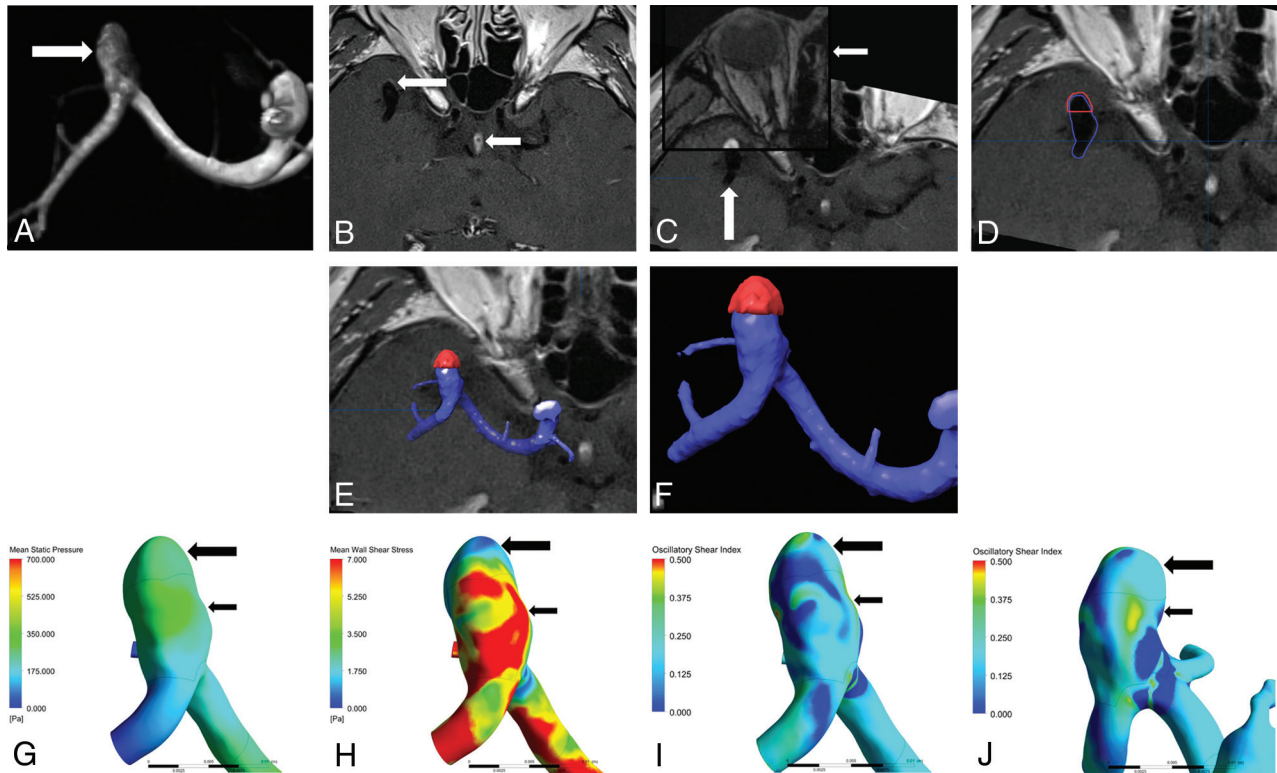


**FIG 2.** A, MRA shows a middle cerebral artery bifurcation aneurysm (*white arrow*). B, Local enhancement on the aneurysmal wall on HR-VWI postgadolinium TIWI (*large white arrow*) compared with that of the pituitary infundibulum (*small white arrow*). C, Auto Fusion of HR-VWI TIWI (*large white arrow*) and TOF-MRA (*small white arrow*) images. D–F, Location of enhanced area (highlighted in red) on the aneurysm (displayed in blue). G, Mean static pressure distribution. H, WSS distribution. The enhanced area has lower mean WSS (*large black arrow*) than the nonenhanced area (*small black arrow*). I and J, OSI distribution. The enhanced area has lower OSI (*large black arrow*) than the nonenhanced area (*small black arrow*).

growing algorithm. Meanwhile, branches extending from the parent artery and the aneurysm were preserved.<sup>9</sup> Then, the vascular models were converted to a stereolithography format and imported into Geomagic Studio 2013 (Geomagic, Research Triangle Park, North Carolina) and SolidWorks 2012 (Dassault Systemes, Waltham, Massachusetts) successively for smoothing, surface construction, cutting off distal redundant arteries along with cutting out vascular inlets and outlets, and keeping the proximal parent artery at least 2 cm long to ensure the numeric stability.

### Computational Fluid Dynamics Analysis

All the aneurysm models were loaded into Fluent Software 17.0 (ANSYS Corporation, Canonsburg, Pennsylvania) for meshing. In addition, the aneurysm wall-enhanced area and the whole aneurysm area were calculated, and the enhanced area ratio was defined as aneurysm wall enhanced area divided by the whole aneurysm area. The enhanced area, nonenhanced area, parent artery, inlets, and outlets of the aneurysm models were selected and defined. Computational fluid dynamics simulations were performed under the transient status, by setting the solver type as pressure-based, the velocity formulation as absolute, and the solver time as transient. The vessel was disposed as a rigid wall with no-slip boundary conditions, neglecting the gravity effect. A laminar and incompressible blood flow, with density and viscosity set as  $1060 \text{ kg/m}^3$  and  $0.004 \text{ Pa} \cdot \text{s}$ , respectively, was used in the calculation.<sup>10</sup> The pulsatile velocity profile of the ICA, which was

obtained from a middle-aged female patient with carotid duplex sonography, was imposed at the inlets, with all the vascular outlets defined as zero pressure boundary conditions. Time-step size was set at 0.02 seconds; the number of time-steps was set at 40. In addition, maximum iterations ranged from 40 to 100. Detailed information about pulsatile ICA velocity can be seen in the Online Appendix.

### Hemodynamic Analysis

Three hemodynamic parameters, which were time-averaged over a cardiac cycle of enhanced area, nonenhanced area, the whole aneurysm, and parent artery, respectively, were calculated, namely mean static pressure (P), mean wall shear stress, and oscillatory shear index (OSI).<sup>8</sup> To compare hemodynamic differences between ruptured and unruptured aneurysms, we calculated the P and WSS of the enhanced area and the whole aneurysm normalized by the parent artery P and WSS.

### Statistical Analysis

Statistical analysis was performed using SPSS 20.0 (IBM, Armonk, New York). The agreement between 2 observers for the presence of local enhancement was evaluated by a  $\kappa$  value. Normally distributed variables were expressed as mean  $\pm$  SD and analyzed with a paired-samples *t* test. Non-normally distributed variables were expressed as the median (interquartile range) and analyzed using a nonparametric paired Wilcoxon rank sum test. Statistical significance was indicated at the .05 level.

**Table 1: Hemodynamic comparison between enhanced and nonenhanced areas<sup>a</sup>**

Variables	Enhanced Area	Nonenhanced Area	P Value <sup>b</sup>
P (Pa)	183.2600 (97.4100–242.9950)	158.8200 (103.5900–220.2000)	.115
WSS (Pa)	3.7255 (1.8487–8.3531)	7.5342 (4.6062–11.1105)	.000 <sup>c</sup>
OSI	0.2288 ± 0.0918	0.3008 ± 0.0890	.021 <sup>c</sup>

<sup>a</sup>Data are expressed as means for normally distributed continuous variables, and as the median for non-normally distributed variables. Numbers in parentheses are interquartile range.

<sup>b</sup>A P value < .05 was statistically significant.

<sup>c</sup>Statistically significant.

**Table 2: Hemodynamic comparison between the whole aneurysm and parent artery<sup>a</sup>**

Variables	Whole Aneurysm	Parent Artery	P Value <sup>b</sup>
P (Pa)	161.4600 (106.7050–220.5200)	181.3400 (104.2630–268.1350)	.313
WSS (Pa)	6.8341 ± 3.7246	9.0612 ± 3.3256	.000 <sup>c</sup>
OSI	0.3402 ± 0.0629	0.2859 ± 0.0560	.007 <sup>c</sup>

<sup>a</sup>Data are expressed as means for normally distributed continuous variables, and as the median for non-normally distributed variables. Numbers in parentheses are interquartile range.

<sup>b</sup>A P value < .05 was statistically significant.

<sup>c</sup>Statistically significant.

## RESULTS

The 2 readers' diagnoses on local enhancement were well-matched ( $\kappa = 0.87$ ). The readers' first and second diagnoses were also consistent ( $\kappa = 0.90$ ). Among 87 patients with 94 aneurysms reviewed, 34 aneurysms had circumferential wall enhancement, while 25 exhibited local enhancement (7 men and 18 women; 8 ruptured and 17 unruptured; mean age, 54.7 years; 8 middle cerebral artery bifurcation aneurysms, 14 posterior communicating artery aneurysms, and 3 ophthalmic artery aneurysms). The aneurysm sizes ranged from 3.2 to 12.9 mm, with a mean enhanced area ratio of 0.37. The number of mean nodes and elements of the aneurysm models were 666,351 and 3,698,735.

### Comparison between Enhanced and Nonenhanced Areas

As is shown in Table 1, the WSS and OSI of the aneurysmal enhanced area were both significantly lower than those of the non-enhanced area (median, 3.7255 vs 7.5342;  $P < .05$ ; mean, 0.2288 ± 0.0918 vs 0.3008 ± 0.0890;  $P = .021$ , respectively). No difference was found regarding mean static pressure.

### Comparison between the Whole Aneurysm and Parent Artery

There were lower WSS (mean, 6.8341 ± 3.7246 vs 9.0612 ± 3.3256;  $P < .05$ ) and higher OSI (mean, 0.3402 ± 0.0629 vs 0.2859 ± 0.0560,  $P = .007$ ) on the whole aneurysm wall than on the parent artery (Table 2). No difference was found regarding mean static pressure.

### Comparison between the Ruptured and Unruptured Aneurysms

There were no statistically significant hemodynamic differences between the ruptured and unruptured aneurysms, either at the enhanced region or on the whole aneurysm (On-line Table).

## DISCUSSION

To our knowledge, our study is the first to reveal the association between hemodynamic characteristics and aneurysm wall enhancement on HR-VWI postgadolinium T1WI.

High-resolution MRI has been used for intracranial aneurysm evaluation and assessment in the past few years.<sup>2,4,11</sup> Several studies have reported the predicting role of high-resolution MRI in distinguishing unstable intracranial aneurysms.<sup>2,4,12</sup> As previ-

ously reported,<sup>13</sup> the aneurysm wall enhancement on HR-VWI postgadolinium T1WI could serve as an independent risk factor for the prediction of aneurysm rupture. On the other hand, hemodynamic forces are believed to act as a prominent factor in aneurysm initiation, progression, and rupture but are poorly understood.<sup>7</sup> Specifically, WSS, one of the most frequently explored but still controversial and puzzling hemodynamic parameters, either high or low, has been shown to be correlated with aneurysm progression and rupture.<sup>7,14,15</sup> However, the hemodynamic characteristics correlated with the enhanced area of the aneurysm wall on HR-VWI post-

gadolinium T1WI have still not been investigated. Therefore, in this study, computational fluid dynamics was performed on aneurysm models generated from 25 patients with local aneurysm enhancement on HR-VWI postgadolinium T1WI, for hemodynamic simulation and parameter calculation.

In our study, the WSS and OSI of the aneurysmal enhanced area were both significantly lower than those of the nonenhanced area (Fig 1H–J and Fig 2H–J). In addition, higher WSS was found in the parent artery in contrast to the whole aneurysm sac due to arterial curvature and tortuosity.<sup>15</sup> The abrupt geometric change caused aneurysm blood turbulence, thus resulting in higher aneurysmal OSI. There were no statistically significant hemodynamic differences between the ruptured and unruptured aneurysms, either at the enhanced region or in the whole aneurysm.

Because WSS is the tangential force exerted by the horizontally moving fluid on the surface<sup>7</sup> and OSI denotes WSS fluctuation magnitude and the tangential force oscillation in a cardiac cycle,<sup>8</sup> low WSS with low OSI may reflect a concentrated blood inflow jet at the enhanced area. We assume that a regional concentrated inflow jet is likely to damage the endothelial cell layer and lead to inflammation, thus changing the aneurysm geometry and promoting its tendency to grow or rupture. In fact, local enhancement of 17 aneurysms in our study was present in the irregularly shaped portions or in daughter sacs, both of which are normally regarded as risk factors for aneurysm rupture. The endothelial damage could possibly cause contrast agent adhesion or uptake or leakage.

Exposure to low WSS has been demonstrated to promote vascular permeability in some studies.<sup>16–18</sup> Conklin et al<sup>16</sup> performed porcine experiments and proposed that low WSS could decrease occludin expression and thus increase vascular permeability. Himborg et al<sup>18</sup> also discovered that being exposed to high WSS, the endothelial permeability to albumin decreased in porcine models. Thus, intra-aneurysmal sites being exposed to low WSS are likely to exhibit elevated permeability to contrast agent, which is presented as local enhancement on HR-VWI postgadolinium T1WI. More advanced studies are needed to confirm this hypothesis.

Several studies also suggested that applying directly to the en-

endothelial cells and acting as a mechanobiological trigger, low WSS may predispose the region to the dysfunction of flow-induced nitric oxide, upregulate endothelial surface adhesion molecules, promote the permeability of endothelial cells, and, thus, facilitate atherosclerotic and inflammatory cell infiltration.<sup>10,14,19-21</sup> Edjlali et al<sup>3</sup> proposed the potential of low WSS in monitoring the aneurysm wall inflammatory process. Hu et al<sup>4</sup> collected a specimen of the aneurysm wall from a patient intraoperatively, which had exhibited local wall enhancement on the high-resolution MRI, and the following histologic study revealed phagocyte and lymphocyte invasion. In our study, we found that the whole aneurysm wall had lower mean WSS than the parent artery. In addition, the enhanced area had lower WSS than the nonenhanced region in the aneurysm as a whole. Low WSS may, therefore, underlie the aneurysm wall local enhancement on HR-VWI postgadolinium T1WI hemodynamically, which is summarized in On-line Fig 4. Future larger studies and further histologic investigation are needed to support this hypothesis.

In an unruptured aneurysm study, low WSS was found to colocalize with thin, easily visualized translucent regions of the aneurysm sac.<sup>22</sup> These regions were thought to be fragile locations of the aneurysm wall that lead to rupture. In addition, in studies on ruptured aneurysms, low WSS was associated with the aneurysm rupture point.<sup>10,20,22,23</sup> In our study, low WSS was also associated with a local enhanced area of the aneurysm wall; the association indicates that the enhanced area may also be the weak part of aneurysm wall. In addition, there were no statistically significant hemodynamic differences between the ruptured and unruptured aneurysms, which indicates that these unruptured aneurysms with local wall enhancement may have a potential risk similar to that of ruptured aneurysms.

### Limitations

In our study, all the aneurysm models were analyzed using the same pulsatile velocity profile of the ICA instead of patient-specific analysis because carotid duplex sonography is not a clinical routine examination. However, it may be able to reflect the hemodynamic differences in various areas of the same model, which we are trying to find. Moreover, we have normalized the aneurysmal values by the parent vessel values to reduce the influence of inlet boundary conditions when making comparisons between different aneurysms.

Moreover, the small number of the patients enrolled into this study may also introduce bias. This may be partly due to the difficulties and risks for patients with unstable and ruptured aneurysms undergoing time-consuming MR imaging examinations. The developing technique discussed here will shorten the examination time and help solve this problem to some extent.

### CONCLUSIONS

The results of this study indicate that hemodynamic differences exist between the enhanced and nonenhanced areas of the aneurysm wall on HR-VWI postgadolinium T1WI. The mean WSS of the aneurysm enhanced area is lower than that of the nonenhanced area, suggesting that low WSS may be an important hemodynamic factor that contributes to the aneurysm wall local

enhancement. In addition, the OSI of the aneurysm enhanced area was lower than that of the nonenhanced area, reflecting a comparatively concentrated inflow jet.

### REFERENCES

1. Matouk CC, Cord BJ, Yeung J, et al. **High-resolution vessel wall magnetic resonance imaging in intracranial aneurysms and brain arteriovenous malformations.** *Top Magn Reson Imaging* 2016;25:49–55 Medline
2. Fu Q, Guan S, Liu C, et al. **Clinical significance of circumferential aneurysmal wall enhancement in symptomatic patients with unruptured intracranial aneurysms: a high-resolution MRI study.** *Clin Neuroradiol* 2017 Jun 27. [Epub ahead of print] CrossRef Medline
3. Edjlali M, Gentric JC, Régent-Rodriguez C, et al. **Does aneurysmal wall enhancement on vessel wall MRI help to distinguish stable from unstable intracranial aneurysms?** *Stroke* 2014;45:3704–06 CrossRef Medline
4. Hu P, Yang Q, Wang DD, et al. **Wall enhancement on high-resolution magnetic resonance imaging may predict an unsteady state of an intracranial saccular aneurysm.** *Neuroradiology* 2016;58:979–85 CrossRef Medline
5. Wang GX, Wen L, Lei S, et al. **Wall enhancement ratio and partial wall enhancement on MRI associated with the rupture of intracranial aneurysms.** *J Neurointerv Surg* 2018;10:566–70 CrossRef Medline
6. Qiu T, Jin G, Bao W, et al. **Intercorrelations of morphology with hemodynamics in intracranial aneurysms in computational fluid dynamics.** *Neurosciences (Riyadh)* 2017;22:205–12 CrossRef Medline
7. Qiu T, Jin G, Xing H, et al. **Association between hemodynamics, morphology, and rupture risk of intracranial aneurysms: a computational fluid modeling study.** *Neurol Sci* 2017;38:1009–18 CrossRef Medline
8. Longo M, Granata F, Racchiusa S, et al. **Role of hemodynamic forces in unruptured intracranial aneurysms: an overview of a complex scenario.** *World Neurosurg* 2017;105:632–42 CrossRef Medline
9. Ren Y, Chen GZ, Liu Z, et al. **Reproducibility of image-based computational models of intracranial aneurysm: a comparison between 3D rotational angiography, CT angiography and MR angiography.** *Biomed Eng Online* 2016;15:50 CrossRef Medline
10. Zhang Y, Jing L, Zhang Y, et al. **Low wall shear stress is associated with the rupture of intracranial aneurysm with known rupture point: case report and literature review.** *BMC Neurol* 2016;16:231 CrossRef Medline
11. Arai D, Satow T, Komuro T, et al. **Evaluation of the arterial wall in vertebralbasilar artery dissection using high-resolution magnetic resonance vessel wall imaging.** *J Stroke Cerebrovasc Dis* 2016;25:1444–50 CrossRef Medline
12. Yalo B, Pop R, Zinchenko I, et al. **Aneurysmal wall imaging in a case of cortical superficial siderosis and multiple unruptured aneurysms.** *BMJ Case Report* 2016;2016 CrossRef Medline
13. Liang F, Qi T, Li F, et al. **High-resolution magnetic resonance vessel wall imaging evaluates intracranial aneurysms: preliminary results.** *Chin J Nerv Ment Dis* 2016;42:175–79
14. Zhang Y, Tian Z, Jing L, et al. **Bifurcation type and larger low shear area are associated with rupture status of very small intracranial aneurysms.** *Front Neurol* 2016;7:169 CrossRef Medline
15. Brinjikji W, Chung BJ, Jimenez C, et al. **Hemodynamic differences between unstable and stable unruptured aneurysms independent of size and location: a pilot study.** *J Neurointerv Surg* 2017;9:376–80 CrossRef Medline
16. Conklin BS, Vito RP, Chen C. **Effect of low shear stress on permeability and occludin expression in porcine artery endothelial cells.** *World J Surg* 2007;31:733–43 CrossRef Medline
17. LaMack JA, Himborg HA, Li XM, et al. **Interaction of wall shear stress magnitude and gradient in the prediction of arterial macromolecular permeability.** *Ann Biomed Eng* 2005;33:457–64 CrossRef Medline
18. Himborg HA, Grzybowski DM, Hazel AL, et al. **Spatial comparison**

- between wall shear stress measures and porcine arterial endothelial permeability.** *Am J Physiol Heart Circ Physiol* 2004;286:H1916–22 CrossRef Medline
19. Sano T, Ishida F, Tsuji M, et al. **Hemodynamic differences between ruptured and unruptured cerebral aneurysms simultaneously existing in the same location: 2 case reports and proposal of a novel parameter oscillatory velocity index.** *World Neurosurg* 2017;98:865–68 CrossRef Medline
  20. Tian Z, Zhang Y, Jing L, et al. **Rupture risk assessment for mirror aneurysms with different outcomes in the same patient.** *Front Neurol* 2016;7:219 CrossRef Medline
  21. Meng H, Tutino VM, Xiang J, et al. **High WSS or low WSS? Complex interactions of hemodynamics with intracranial aneurysm initiation, growth, and rupture: toward a unifying hypothesis.** *AJNR Am J Neuroradiol* 2014;35:1254–62 CrossRef Medline
  22. Kadasi LM, Dent WC, Malek AM. **Colocalization of thin-walled dome regions with low hemodynamic wall shear stress in unruptured cerebral aneurysms.** *J Neurosurg* 2013;119:172–79 CrossRef Medline
  23. Miura Y, Ishida F, Umeda Y, et al. **Low wall shear stress is independently associated with the rupture status of middle cerebral artery aneurysms.** *Stroke* 2013;44:519–21 CrossRef Medline